Linear instability of the Darcy–Hadley flow in an inclined porous layer

A. Barletta[1,a)] and D. A. S. Rees[2,b)]
[1]*DIENCA, Alma Mater Studiorum – Università di Bologna, Viale Risorgimento 2, I–40136 Bologna, Italy*
[2]*Department of Mechanical Engineering, University of Bath, Claverton Down, Bath BA2 7AY, United Kingdom*

(Received 23 April 2012; accepted 18 June 2012; published online 10 July 2012)

The buoyant flow in a saturated porous layer inclined to the horizontal is studied under the assumption that the plane impermeable boundaries are subject to linear temperature distributions up the layer. The basic solution is stationary and such that the temperature gradient is inclined to the boundary walls. Two parameters govern the thermal boundary conditions: the Rayleigh number, associated with the component of the basic temperature gradient orthogonal to the boundaries, the Hadley-Rayleigh number, associated with the component of the basic temperature gradient parallel to the boundaries. The linear stability of the basic solution with respect to the longitudinal normal modes is studied by employing two different numerical methods: a collocation method of weighted residuals, and a Runge–Kutta solver. Different regimes are considered: the upward–cooling condition, the upward–heating condition, and the buoyancy–balanced condition. The latter regime implies a vanishing velocity distribution and a vertical temperature gradient in the basic state. In the upward–cooling regime, for a fixed Hadley–Rayleigh number, the increasing inclination to the horizontal leads to a destabilising effect. When the inclination exceeds a threshold angle that depends on the Hadley–Rayleigh number, the basic solution becomes unstable for every Rayleigh number. The reverse holds true in the upward–heating regime, where the increasing inclination to the horizontal stabilises the basic flow. The general oblique normal modes are finally considered. It is shown that the longitudinal modes are selected at the onset of convection, except for the case of the Darcy–Bénard limiting case where all the oblique modes are equivalent.
 [http://dx.doi.org/10.1063/1.4732781]

I. INTRODUCTION

The stability analysis of fluid layers or fluid saturated porous layers heated from below allows one to determine the conditions when convection initiates. If a stationary basic flow is examined, the convective instability emerges as a secondary flow superposed onto the basic flow.

Among the many circumstances where the mechanism of heating from below may arise, the one in which we are interested is a plane saturated porous layer which is inclined to the horizontal, a problem originally investigated by Bories and Combarnous,[1] by Weber,[2] and by Caltagirone and Bories.[3] These authors assumed unequal uniform temperatures on the boundary surfaces and found that instability occurs when the Rayleigh number exceeds $4\pi^2/\cos\phi$, where ϕ is the inclination angle above the horizontal. The long–standing issue of pattern selection, i.e., whether polygonal cells or longitudinal rolls occur at the onset of convective instability has been revisited recently in a note by Nield.[4] Additional results were obtained by Rees and Bassom,[5] who defined a transformation which

a)antonio.barletta@unibo.it.
b)ensdasr@bath.ac.uk.

maps arbitrary three–dimensional normal modes (oblique rolls) into two–dimensional normal modes (transverse rolls). These authors proved that the transverse rolls are allowed only if the inclination angle ϕ above the horizontal is smaller than 31.49032°. A detailed survey of the literature on this subject may be found in Nield and Bejan.[6] Recently, Nield, Barletta, and Celli[7] included the effect of viscous dissipation in the analysis of the conditions for the onset of the instability. Further recent results were reported by Barletta and Storesletten[8] and by Rees and Barletta.[9] These authors investigated the effects of assuming Neumann boundary conditions for the temperature field, instead of Dirichlet boundary conditions.

In addition to the uniform temperature (Dirichlet) boundary conditions, and the uniform heat flux (Neumann) boundary conditions, another classical boundary condition is given by the assumption of a steady boundary temperature which varies linearly along the boundary. This boundary condition can be important, for instance, in modelling the compact heat exchangers based on metal foams or in the applications relative to geological media.[10] For a horizontal layer, linearly varying boundary temperatures give rise to a Hadley circulation in the basic state. The name Hadley circulation is after George Hadley, an English meteorologist of the eighteenth century. Weber[11] considered a basic state of Hadley circulation in a study of the onset of convection in a horizontal porous layer modelled through Darcy's law. Later developments of this subject were achieved by Nield,[12] by Nield, Manole, and Lage,[13] by Nield,[14] by Kaloni and Qiao[15] and by Nield.[16] Recent studies on the stability of the Darcy–Hadley flow have been carried out by including the effects of a vertical throughflow[17,18] or the combined effects of pressure work and viscous dissipation.[19] The concurrent action of heat and solutal diffusion has been investigated by Diaz and Brevdo.[20]

To the best of the authors' knowledge, all the studies related to the Darcy–Hadley flow published to date are relative to a horizontal layer. The aim of the present study is to extend the analysis to the case of a porous layer inclined to the horizontal. Thus, we aim to consider a general problem that includes both the special case of an inclined porous layer with uniform boundary temperatures, and the special case of the Darcy–Hadley flow in a horizontal porous layer. The linearly varying boundary temperatures imply, in the case of an inclined layer, that two different regimes exist, as the temperature may increase or decrease up the slope. The stability of the basic Darcy–Hadley flow in an inclined layer to small–amplitude disturbances will be analysed numerically by employing a collocation method of weighted residuals and a Runge–Kutta solver.

II. MATHEMATICAL MODEL

Let us consider a porous layer inclined to the horizontal, where the inclination angle is ϕ. We assume that the boundaries are impermeable and subject to nonuniform linear temperature distributions, such that the dimensionless boundary conditions can be expressed as

$$\begin{aligned} y = 0: &\qquad v = 0, \quad T = 1 - \lambda x, \\ y = 1: &\qquad v = 0, \quad T = -\lambda x. \end{aligned} \tag{1}$$

A sketch of the porous layer is drawn in Fig. 1, where $\mathbf{g}$ denotes the gravitational acceleration. The dimensionless quantities are defined such that

$$\begin{aligned} &\frac{1}{L}\,\mathbf{x}^* = \frac{1}{L}\left(x^*, y^*, z^*\right) = (x, y, z) = \mathbf{x}, \\ &\frac{L}{\alpha}\,\mathbf{u}^* = \frac{L}{\alpha}\left(u^*, v^*, w^*\right) = (u, v, w) = \mathbf{u}, \\ &\frac{\alpha}{\sigma L^2}\,t^* = t, \quad \frac{T^* - T_0}{\Delta T} = T, \end{aligned} \tag{2}$$

where the starred symbols are the dimensional fields, coordinates, and time. The average thermal diffusivity is α, the layer thickness is L, the ratio between the volumetric heat capacity of the saturated porous medium, and the volumetric heat capacity of the fluid is σ. We denoted by T_0 and ΔT the reference temperature and the reference temperature difference, considered as positive, associated with the thermal boundary conditions. The dimensionless constant λ appearing in

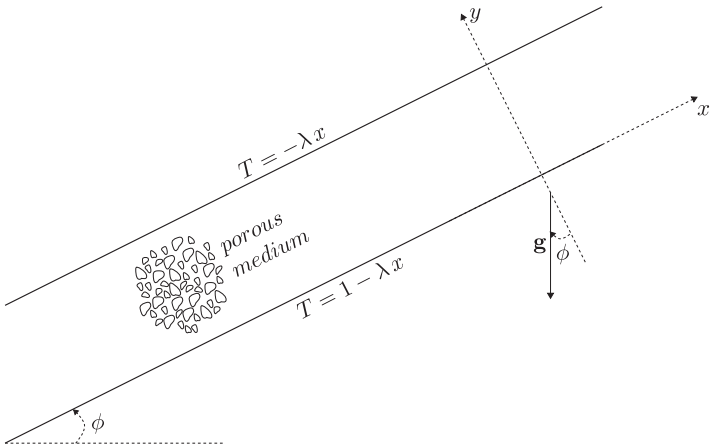

FIG. 1. Sketch of the inclined porous layer.

Eq. (1) is obtained dividing the dimensional wall temperature gradient along the x–direction by the constant $\Delta T/L$.

We assume the validity of Darcy's law, as well as of the Oberbeck–Boussinesq approximation. We further assume that the solid and fluid phases are in local thermal equilibrium, and that internal heating or viscous dissipation effects are absent or negligible.

Thus, the governing equations can be expressed in a dimensionless form as

$$\boldsymbol{\nabla} \cdot \mathbf{u} = 0, \tag{3a}$$

$$\boldsymbol{\nabla} \times \mathbf{u} = R\, \boldsymbol{\nabla} \times [T(\sin\phi\, \hat{\mathbf{e}}_x + \cos\phi\, \hat{\mathbf{e}}_y)], \tag{3b}$$

$$\frac{\partial T}{\partial t} + (\mathbf{u} \cdot \boldsymbol{\nabla})\, T = \nabla^2 T. \tag{3c}$$

Here, R is the Darcy–Rayleigh number defined as

$$R = \frac{g\beta \Delta T K L}{\nu \alpha}, \tag{4}$$

where K is the permeability of the porous medium and ν is the kinematic viscosity of the fluid. We note that Eq. (3b) was obtained by evaluating the curl of the local momentum balance equation. The effects of heterogeneity in the porous medium have been neglected; recent studies on the stability analysis in heterogeneous porous media have been carried out by Barletta, Celli, and Kuznetsov.[21,22]

III. THE INCLINED HADLEY FLOW

A basic solution of Eqs. (3) is obtained for a steady–state, with purely parallel throughflow along the x–direction,

$$u_b = \frac{1}{2}\, R\, (\lambda \cos\phi - \sin\phi)\, \frac{\sin[(2y-1)\,\Omega/2]}{\sin(\Omega/2)}, \quad v_b = 0, \quad w_b = 0, \tag{5a}$$

$$T_b = -\lambda x + \frac{1}{2}\big[1 + \lambda\,(1-2y)\cot\phi + \cos(\Omega y)\,(1 - \lambda\cot\phi) - (1 - \lambda\cot\phi)\cot(\Omega/2)\sin(\Omega y)\big], \tag{5b}$$

where "b" stands for "basic solution," and

$$\Omega = \sqrt{\lambda R \sin\phi}. \tag{6}$$

Equation (5a) describes a velocity profile with a vanishing mass flow rate.

Two limiting cases are specially interesting: the limit $\lambda \to 0$, namely the limit of an inclined channel with uniform wall temperatures; the limit $\phi \to 0$, namely the limit of the horizontal Hadley flow.

In the limit $\lambda \to 0$, Eqs. (5) and (6) yield

$$u_b = \left(\frac{1}{2} - y\right) R \sin\phi, \quad v_b = 0, \quad w_b = 0, \tag{7a}$$

$$T_b = 1 - y, \tag{7b}$$

in perfect agreement with the basic solution considered in Rees and Bassom.[5]

In the limit $\phi \to 0^\circ$, Eqs. (5) and (6) yield

$$u_b = \left(y - \frac{1}{2}\right) \lambda R, \quad v_b = 0, \quad w_b = 0, \tag{8a}$$

$$T_b = 1 - \lambda x - y - \frac{\lambda^2 R}{12}\left(y - 3y^2 + 2y^3\right), \tag{8b}$$

in perfect agreement with the basic solution reported in Section 7.9 of the book by Nield and Bejan.[6]

We mention that hereafter R will be considered as positive, with $\phi \in [0^\circ, 90^\circ]$. On the other hand, λ can be either positive (wall temperature decreasing up the layer) or negative (wall temperature increasing up the layer). When $\lambda < 0$, the parameter Ω becomes purely imaginary, but Eqs. (5) can still be used provided that the trigonometric functions containing Ω in their argument are replaced by hyperbolic functions.

A special feature of the Hadley flow with $\lambda > 0$ is that, as it can be inferred from Eqs. (5) and (6), the basic solution becomes singular when

$$\sin\phi = \frac{4n^2\pi^2}{\lambda R}, \qquad n = 1, 2, 3, \ \ldots \ . \tag{9}$$

These singularities are displayed for sufficiently high values of the product λR. This product is, in fact, the Hadley–Rayleigh number,

$$R_H = \lambda R. \tag{10}$$

The dimensionless parameter R_H is usually called horizontal Rayleigh number in the classical formulation of the Hadley flow problem relative to a horizontal layer (see, for instance, Nield and Bejan[6]). Here, the streamwise direction is not the horizontal, since the layer is inclined, thence we prefer the term Hadley–Rayleigh number. We point out that R is chosen as positive, meaning that the lower boundary wall is hotter than the upper boundary wall for any fixed cross–section $x = constant$. On the other hand R_H can be either positive or negative leading to different features of the basic solution and of the stability analysis of this solution,

$$R_H > 0, \qquad \text{upward–cooling regime},$$

$$R_H < 0, \qquad \text{upward–heating regime}.$$

The singularities defined by Eq. (9) exist for the upward–cooling flow when $R_H > 4\pi^2$. They define conditions where no parallel flow solution with a vanishing mass flow rate is allowed.

Another interesting feature of the upward–cooling regime is the existence of a special basic state where the fluid is at rest ($u_b = v_b = w_b = 0$), and the temperature profile is just the conduction profile, $T_b = 1 - \lambda x - y$. This feature can be inferred from Eqs. (5). In fact, one has $u_b = 0$ identically, and $T_b = 1 - \lambda x - y$ when $\lambda = \tan\phi$, and this means

$$R_H = R \tan\phi. \tag{11}$$

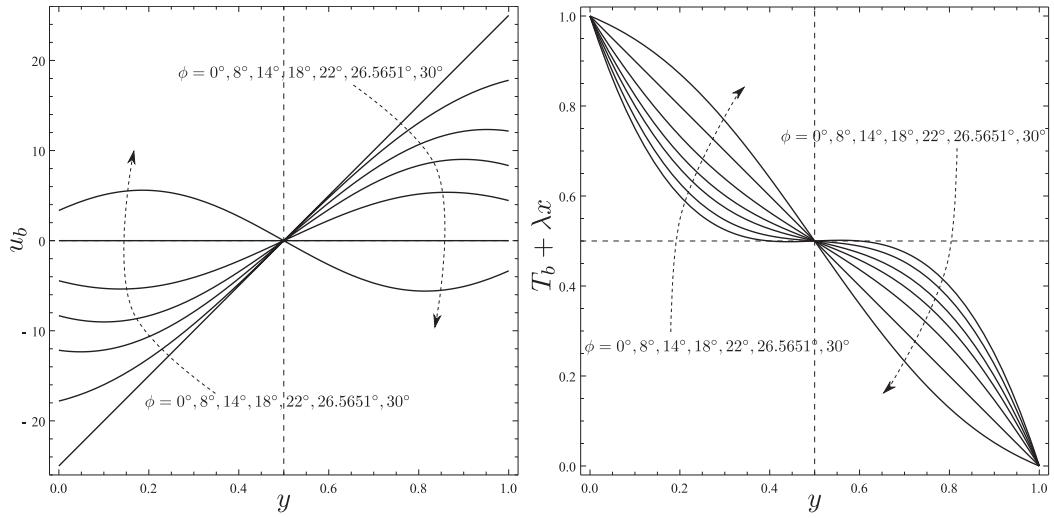

FIG. 2. Upward–cooling basic flow: Plots of u_b and of $T_b + \lambda x$ versus y, for $R = 100$ and $R_H = 50$.

Equation (11) defines a special upward–cooling regime where the basic state is just the same that would exist if the porous layer were horizontal ($\phi \to 0°$). Hereafter, this special basic state will be called the buoyancy–balanced rest state. In fact, the buoyancy–balanced rest state occurs when the basic temperature gradient is perfectly parallel to the gravitational acceleration, that is when ∇T_b is vertical.

Figures 2 and 3 show the basic velocity profiles and the basic temperature profiles for increasing inclinations above the horizontal; reference is made to a upward–cooling case ($R = 100$, $R_H = 50$, Fig. 2), and to a upward–heating case ($R = 200$, $R_H = -50$, Fig. 3). Figure 2 illustrates the behaviour when the buoyancy–balanced rest state ($\phi = \arctan \frac{1}{2} = 26.5651°$) is exceeded. We see that the transition from $\phi = 22°$ to $\phi = 30°$ implies a change in the direction of the single–cell basic flow from co–rotating to counter–rotating, passing from a rest state ($\phi = 26.5651°$). In the upward–heating case (Fig. 3), the increasing inclination yields higher velocity gradients close to the boundary walls.

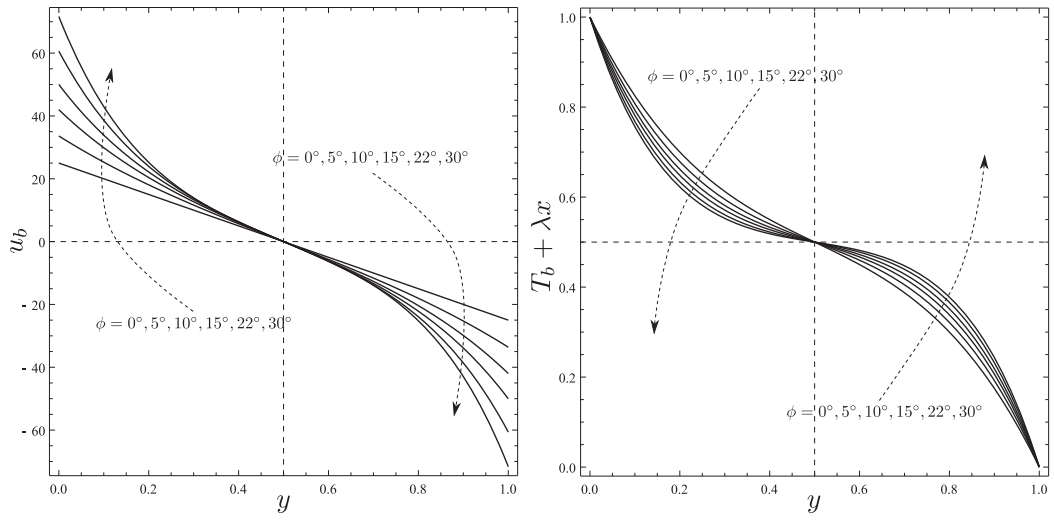

FIG. 3. Upward–heating basic flow: Plots of u_b and of $T_b + \lambda x$ versus y, for $R = 200$ and $R_H = -50$.

IV. LINEAR DISTURBANCES

We now perturb the basic solution, Eqs. (5), by defining

$$(u, v, w) = (u_b, v_b, w_b) + \varepsilon(U, V, W), \qquad T = T_b + \varepsilon\theta, \tag{12}$$

where ε is a small perturbation parameter. Substitution of Eq. (12) in Eqs. (3) yields

$$\frac{\partial U}{\partial x} + \frac{\partial V}{\partial y} + \frac{\partial W}{\partial z} = 0, \tag{13a}$$

$$\frac{\partial W}{\partial y} - \frac{\partial V}{\partial z} = -R\,\frac{\partial \theta}{\partial z}\,\cos\phi, \tag{13b}$$

$$\frac{\partial U}{\partial z} - \frac{\partial W}{\partial x} = R\,\frac{\partial \theta}{\partial z}\,\sin\phi, \tag{13c}$$

$$\frac{\partial V}{\partial x} - \frac{\partial U}{\partial y} = R\,\frac{\partial \theta}{\partial x}\,\cos\phi - R\,\frac{\partial \theta}{\partial y}\,\sin\phi, \tag{13d}$$

$$\frac{\partial \theta}{\partial t} + u_b(y)\,\frac{\partial \theta}{\partial x} - \lambda U - F(y)\,V = \nabla^2\theta, \tag{13e}$$

where the terms $O(\varepsilon^2)$ have been neglected, and where

$$F(y) = -\frac{\partial T_b}{\partial y} = \lambda\cot\phi + \frac{\Omega}{2}\sin(\Omega y)\,(1 - \lambda\cot\phi) + \frac{\Omega}{2}\,(1 - \lambda\cot\phi)\cot(\Omega/2)\cos(\Omega y). \tag{14}$$

Equations (13) are subject to the boundary conditions implied by Eqs. (1) and (12), namely

$$y = 0, 1: \qquad V = 0, \quad \theta = 0. \tag{15}$$

V. LONGITUDINAL ROLLS

We now consider linear disturbances such that (U, V, W, θ) are independent of x. Then, Eq. (13a) can be identically satisfied by defining a streamfunction $\psi(y, z, t)$ such that

$$V(y, z, t) = \frac{\partial \psi(y, z, t)}{\partial z}, \qquad W(y, z, t) = -\frac{\partial \psi(y, z, t)}{\partial y}. \tag{16}$$

Thus, Eqs. (13) yield

$$\nabla^2\psi = R\,\frac{\partial \theta}{\partial z}\,\cos\phi, \tag{17a}$$

$$U = R\,\theta\,\sin\phi + S(t), \tag{17b}$$

$$\frac{\partial \theta}{\partial t} - \lambda U - F(y)\,\frac{\partial \psi}{\partial z} = \nabla^2\theta, \tag{17c}$$

where $S(t)$ is an arbitrary function of time. We assume normal mode disturbances,

$$\begin{Bmatrix} U(y, z, t) \\ \psi(y, z, t) \\ \theta(y, z, t) \end{Bmatrix} = \begin{Bmatrix} a(y) \\ if(y) \\ h(y) \end{Bmatrix} \exp[i\,(kz - \omega t)]\,. \tag{18}$$

We point out that, on the right hand side of Eq. (18), one must consider only the real part in order to find the expressions of (U, ψ, θ). In Eq. (17), k is the wavenumber and ω is a complex parameter. If $\Im\mathrm{m}\{\omega\} > 0$, we have instability, while if $\Im\mathrm{m}\{\omega\} < 0$, we have stability. In the following, we will be interested in determining the neutral stability condition, so that we will set $\Im\mathrm{m}\{\omega\} = 0$. Equation (17b) is consistent with Eq. (18), for $k \neq 0$, only if $S(t)$ is chosen as identically vanishing. Thus, Eqs. (10), (17) and (18) lead to the eigenvalue problem

$$f'' - k^2 f - Rkh\cos\phi = 0, \tag{19a}$$

$$h'' + \left(i\omega - k^2 + R_H \sin\phi\right) h - kF(y) f = 0, \tag{19b}$$

$$y = 0, 1: \qquad f = 0, \quad h = 0. \tag{19c}$$

Equation (19c) has been obtained from Eq. (15). The exchange of stabilities holds (a proof is given in the Appendix) so that $\omega = 0$, i.e., only the stationary longitudinal rolls exist. Thus, Eqs. (19) simplify to

$$f'' - k^2 f - Rkh\cos\phi = 0, \tag{20a}$$

$$h'' - \left(k^2 - R_H \sin\phi\right) h - kF(y) f = 0, \tag{20b}$$

$$y = 0, 1: \qquad f = 0, \quad h = 0. \tag{20c}$$

A. Numerical solution

We now adopt the collocation method of weighted residuals and express the eigenfunctions $f(y)$ and $h(y)$ so that Eq. (19c) is satisfied,

$$f(y) = \sum_{n=1}^{N} f_n \sin(n\pi y), \quad h(y) = \sum_{n=1}^{N} h_n \sin(n\pi y). \tag{21}$$

On substituting in Eq. (20a) we obtain

$$h_n = -\frac{n^2\pi^2 + k^2}{Rk\cos\phi} f_n, \qquad n = 1, 2, \ \ldots \ N, \tag{22}$$

and Eq. (20b) yields the residual

$$E(y) = \sum_{n=1}^{N} \left[\left(n^2\pi^2 + k^2 - R_H \sin\phi\right) \frac{n^2\pi^2 + k^2}{Rk\cos\phi} - kF(y) \right] f_n \sin(n\pi y). \tag{23}$$

We prescribe that $E(y)$ vanishes at the collocation points $y = y_m$, where

$$y_m = \frac{m}{N+1}, \quad m = 1, 2, \ \ldots \ , N. \tag{24}$$

Thus, the equation $E(y_m) = 0$, for $m = 1, 2, \ldots, N$, form a system of N homogeneous linear equations in the unknowns $(f_1, f_2, \ldots, f_N)$. We can write this system in matrix form,

$$\mathbb{M} \cdot \mathbb{f} = 0, \tag{25}$$

where

$$\begin{aligned} \mathbb{M}_{mn} &= \left[\left(n^2\pi^2 + k^2 - R_H \sin\phi\right) \frac{n^2\pi^2 + k^2}{Rk\cos\phi} - kF(y_m) \right] \sin(n\pi y_m), \\ \mathbb{f}_n &= f_n, \qquad m, n = 1, 2, \ \ldots \ , N. \end{aligned} \tag{26}$$

The solution of the eigenvalue problem Eqs. (20) is obtained by prescribing

$$\det(\mathbb{M}) = 0, \tag{27}$$

so that nontrivial solutions $\mathbb{f}$ of Eq. (25) are allowed.

The neutral stability curves $R(k)$ are obtained, for any fixed pair (ϕ, R_H) by solving Eq. (27). We must fix the number N of collocation points, and we checked that, in all the cases discussed hereafter, a number $N \leq 8$ is perfectly adequate for a reliable graphical representation of the neutral stability curves. We also used a numerical solution of Eqs. (20) based on the Runge–Kutta method and on the shooting method (see, for instance, Barletta and Rees[23] for a detailed description) to obtain a validation of the results.

Equation (27) is in fact an algebraic equation of degree N in the unknown $R(k)$. Geometrically, the multiplicity of the solutions means that the neutral stability condition displays several branches. All these branches can be represented by means of the function `ContourPlot` within the application *Mathematica 8*. The use of the function `ContourPlot` requires specification of a rectangular domain in the (k, R)–plane. All Figs. 4–7 have been drawn by this method. The rectangular domain in the (k, R)–plane has been chosen so that only the lower branch $R(k)$ appears, for every choice of ϕ and R_H.

B. The neutral stability curves

Figures 4–6 display the neutral stability curves for upward–cooling basic flows with $R_H \leq 60$, while Fig. 7 is relative to upward–heating basic flows with $R_H = -10, -20, -30$. In a horizontal porous layer, the longitudinal temperature gradient has a stabilizing effect,[6,19] except for very large values of R_H exceeding approximately 80. When the basic solution is with upward–heating, Fig. 7 reveals a similar behaviour also for an inclined layer. We can well say that the stabilizing effect of the longitudinal temperature gradient acts synergically, in this case, with the stabilizing effect of the inclination.

A deeply different behaviour is observed in the upward–cooling regime. Figures 4–6 show that the effect of an increasing R_H is strongly dependent on ϕ. We see that the neutral stability curves for $R_H > 0$ gradually fall below the curve for $R_H \to 0$, meaning a destabilizing effect. For $R_H = 30$, the destabilization means a linear instability for every R when ϕ moves from 19.2° to 19.3°. This effect is caused by the behaviour of the neutral stability curve relative to $R_H = 30$ when $k \to 0$. What happens with $R_H = 30$ and $\phi = 19.2^\circ$ is observed also with $R_H = 20$ and $\phi = 29.5^\circ$ (Fig. 4), and eventually with $R_H = 10$ and $\phi = 80.7^\circ$. If we consider higher values of R_H (Fig. 6) the destabilization of the basic flow for every R takes place at smaller inclination angles: 9.4° for $R_H = 60$; 11.3° for $R_H = 50$; 14.2° for $R_H = 40$. For a prescribed R_H, the threshold angle is the value of ϕ such that, when this value is exceeded, the basic solution is unstable to longitudinal rolls for every positive value of R.

The threshold angles $\phi = 9.4^\circ$, $\phi = 11.3^\circ$, $\phi = 14.2^\circ$, $\phi = 19.2^\circ$, $\phi = 29.5^\circ$, and $\phi = 80.7^\circ$ detected numerically for $R_H = 60, 50, 40, 30, 20, 10$, respectively, can also be obtained analytically. This can be done by employing a perturbation expansion of the eigenfunctions f and h for small wave numbers k. From Eqs. (20), one obtains that, in the limit $k \to 0$, the lowest mode of neutral stability is

$$h(y) = C\sin(\pi y), \qquad f(y) = 0, \tag{28}$$

where C is an arbitrary integration constant. This mode exists only if ϕ and R_H satisfy the relationship

$$\phi = \arcsin\left(\frac{\pi^2}{R_H}\right). \tag{29}$$

Equation (29) allows one to determine with a high accuracy the threshold angles for $R_H = 60, 50, 40, 30, 20, 10$; one obtains $\phi = 9.46781^\circ$, $\phi = 11.3845^\circ$, $\phi = 14.2847^\circ$, $\phi = 19.2073^\circ$, $\phi = 29.5696^\circ$ and $\phi = 80.7372^\circ$, respectively.

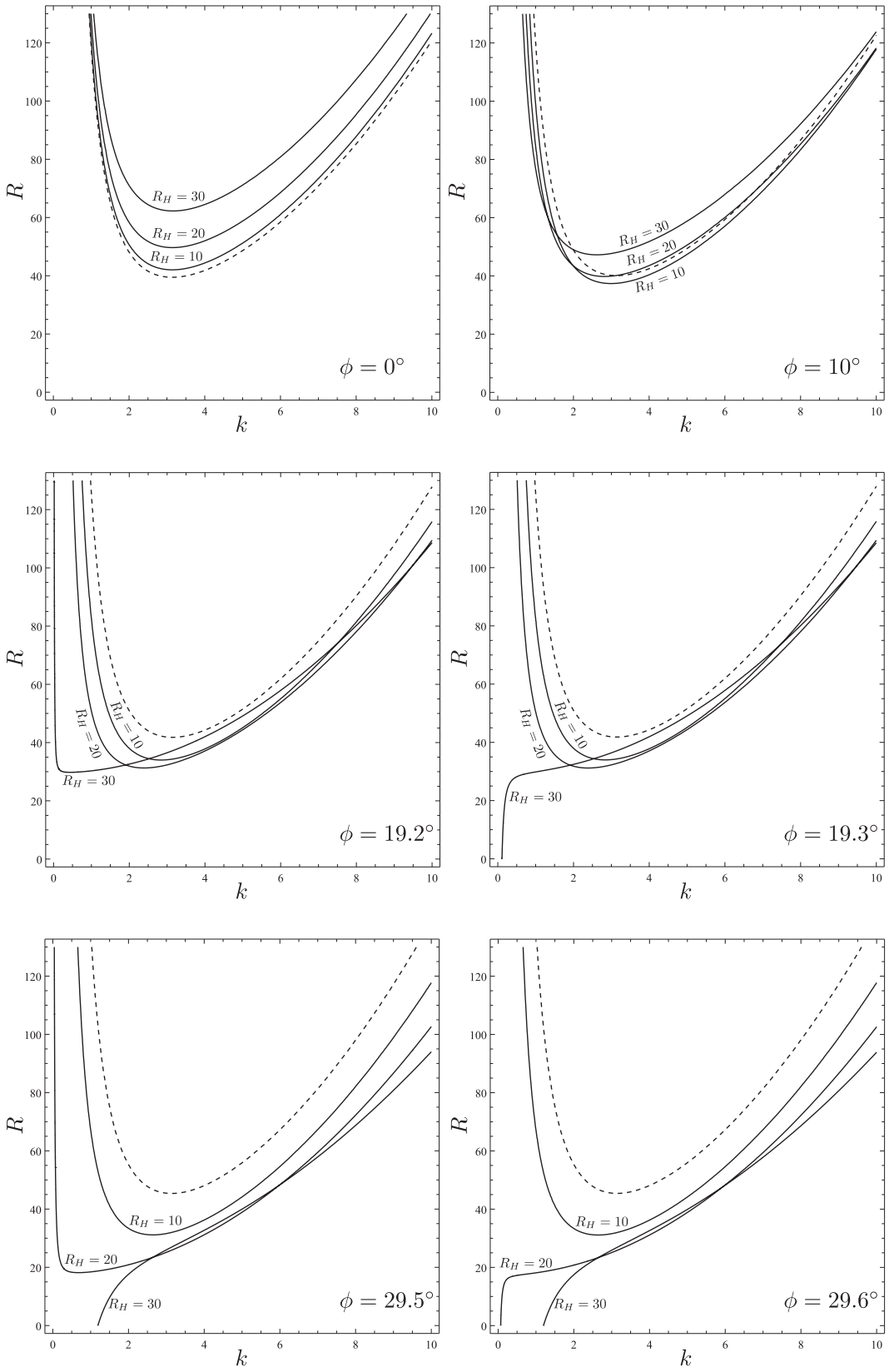

FIG. 4. Longitudinal rolls: Neutral stability curves $R(k)$ for $R_H = 10, 20, 30$. and increasing inclination angles ϕ; the dashed curves are for $R_H \to 0$.

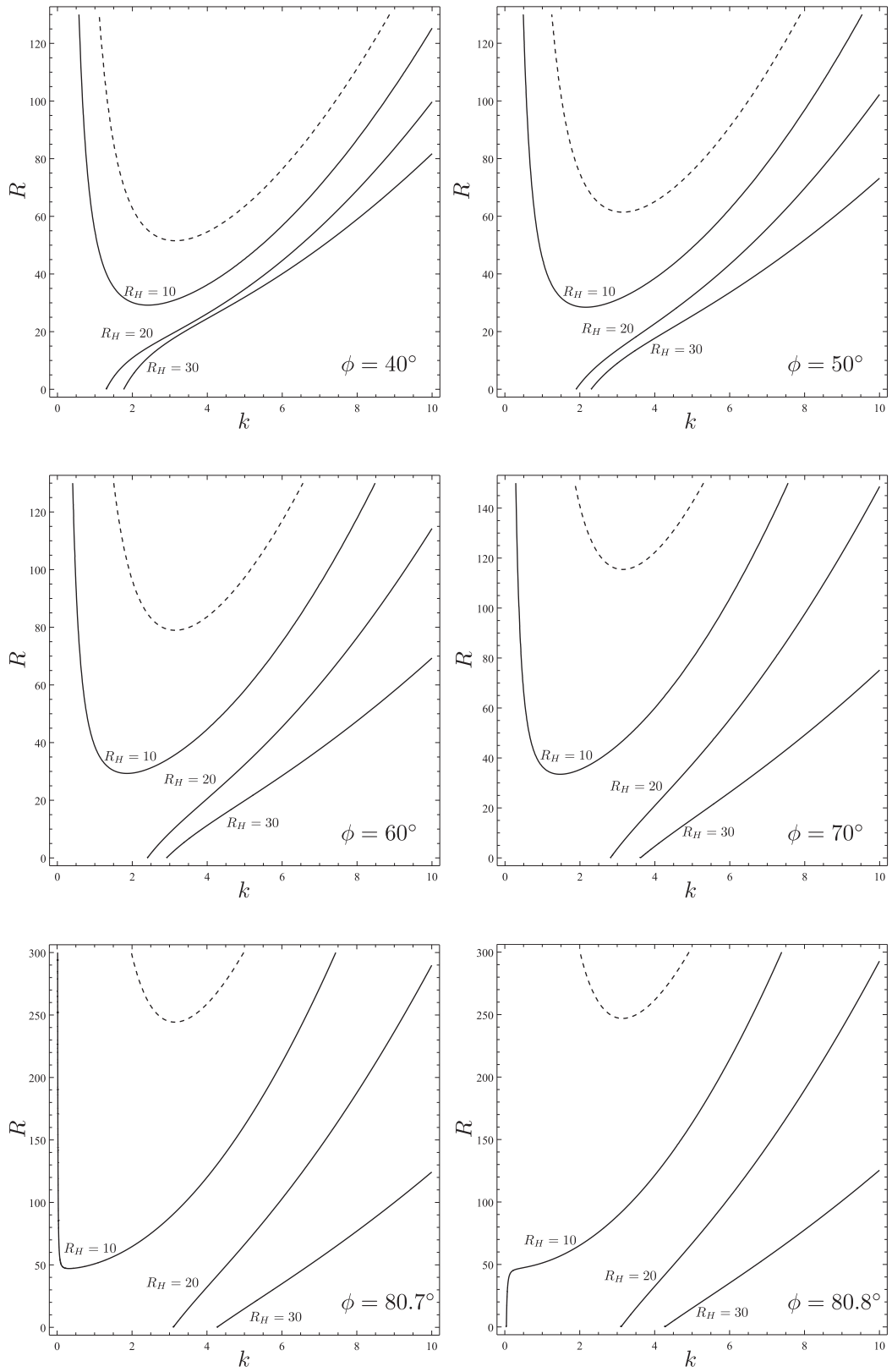

FIG. 5. Longitudinal rolls: Neutral stability curves $R(k)$ for $R_H = 10$, 20, 30. and increasing inclination angles ϕ; the dashed curves are for $R_H \to 0$.

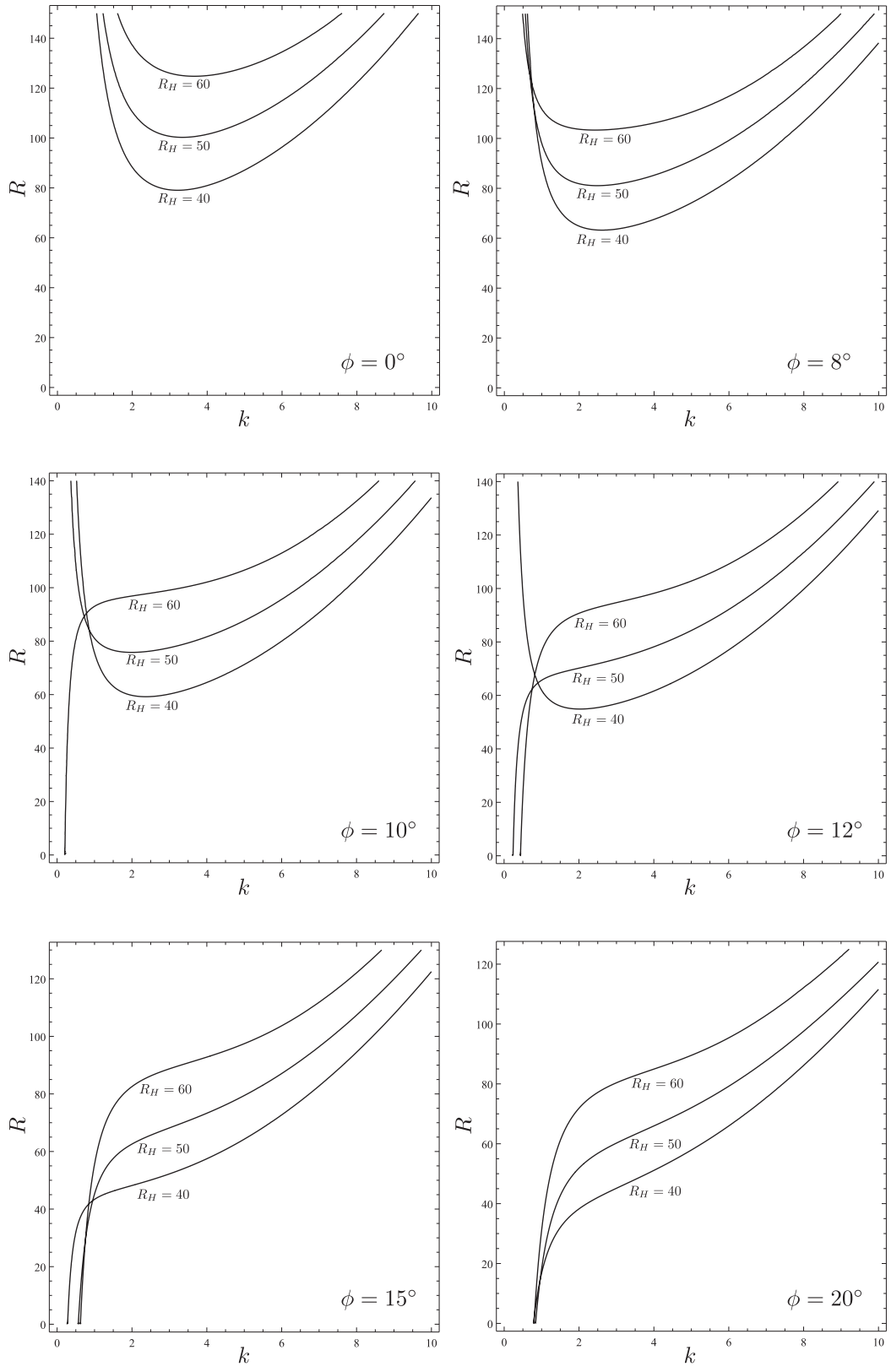

FIG. 6. Longitudinal rolls: Neutral stability curves $R(k)$ for $R_H = 40$, 50, 60, and increasing inclination angles ϕ.

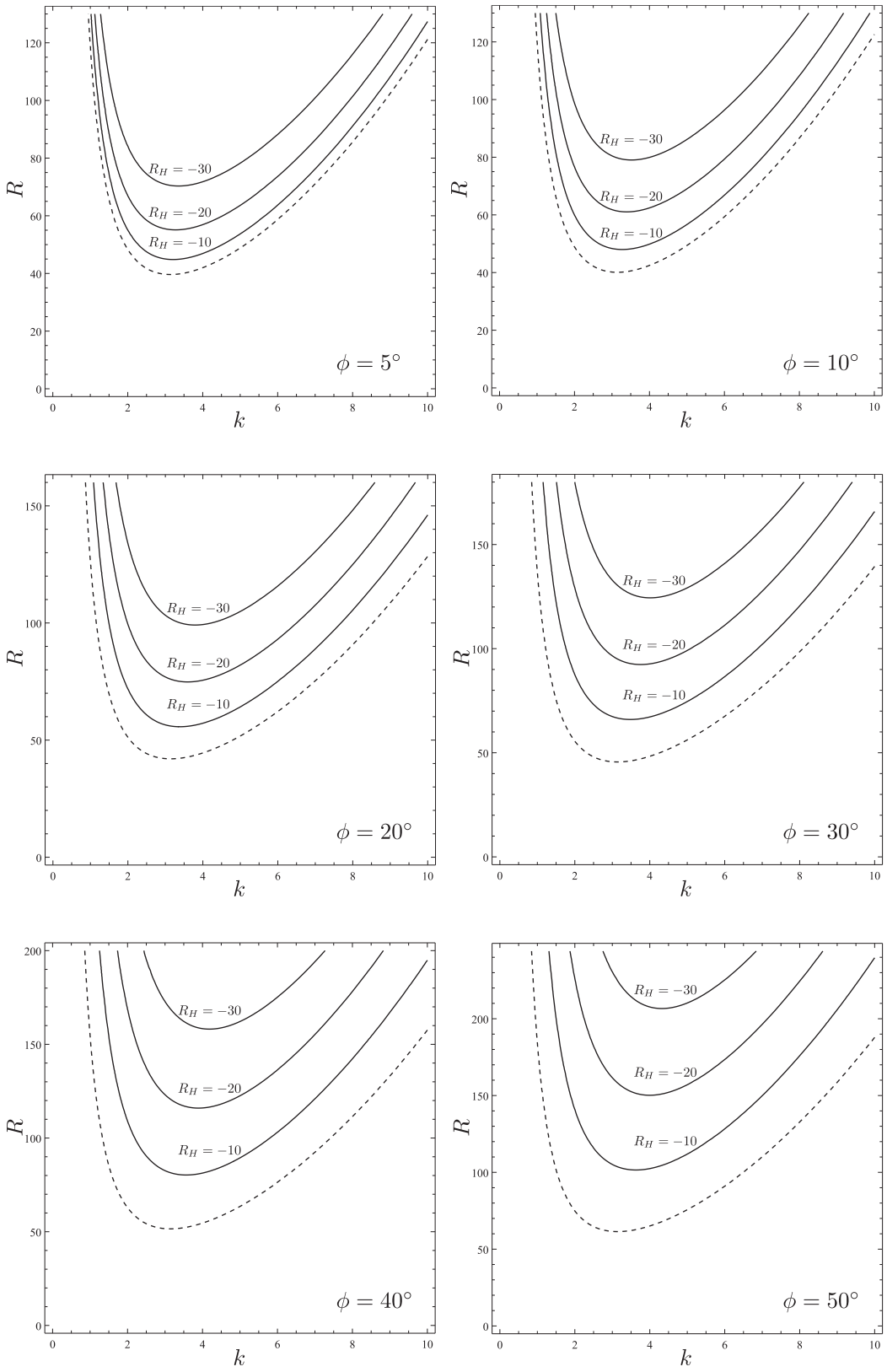

FIG. 7. Longitudinal rolls: Neutral stability curves $R(k)$ for $R_H = -10, -20, -30$ and increasing inclination angles ϕ; the dashed curves are for $R_H \to 0$.

C. Stability of the buoyancy–balanced rest state

If R_H depends on R through Eq. (11), Eqs. (10) and (14) imply $F(y) = 1$. Thus, the eigenvalue problem Eqs. (20) can be rewritten as

$$f'' - k^2 f - Rkh\cos\phi = 0, \tag{30a}$$

$$h'' - \left(k^2 - R\tan\phi\sin\phi\right) h - kf = 0, \tag{30b}$$

$$y = 0, 1: \qquad f = 0, \quad h = 0. \tag{30c}$$

In this special case, the Fourier modes defined by Eq. (21) are independent, so that Eq. (20b) is satisfied with

$$\left(n^2\pi^2 + k^2 - R\tan\phi\sin\phi\right)\frac{n^2\pi^2 + k^2}{Rk\cos\phi} - k = 0, \tag{31}$$

and this yields the neutral stability condition

$$R(k) = \frac{\left(k^2 + n^2\pi^2\right)^2\cos\phi}{k^2 + n^2\pi^2\sin^2\phi}. \tag{32}$$

The least stable mode is $n = 1$. Thus, the critical values of k and R for the onset of the instability are given by

$$k_c = \begin{cases} \pi\sqrt{\cos(2\phi)}, & 0^\circ \le \phi \le 45^\circ \\ 0, & 45^\circ < \phi < 90^\circ \end{cases}, \qquad R_c = \begin{cases} 4\pi^2\cos^3\phi, & 0^\circ \le \phi \le 45^\circ \\ \pi^2\cot\phi\csc\phi, & 45^\circ < \phi < 90^\circ \end{cases}. \tag{33}$$

We mention that Eqs. (32) and (33) are consistent with the classical solution of the Darcy–Bénard problem,[6,24–26] that is the stability analysis of the rest state in a horizontal layer ($\phi = 0^\circ$).

Figure 8 displays the neutral stability curves for the least stable mode, $n = 1$, and relative to different inclination angles ϕ. Figure 9 illustrates the change of k_c and R_c versus ϕ. The general conclusion is that the buoyancy–balanced rest state becomes more and more unstable as the inclination above the horizontal increases. When $\phi \to 90^\circ$, the neutral stability curve $R(k)$ flattens to zero so that $R_c \to 0$.

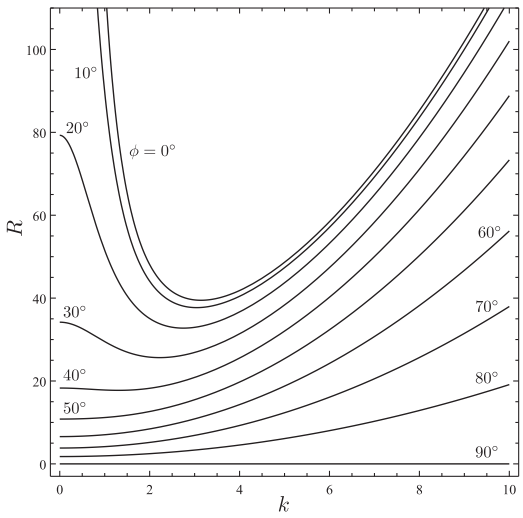

FIG. 8. Longitudinal rolls: Neutral stability curves $R(k)$ for the buoyancy–balanced rest state at different inclinations ϕ.

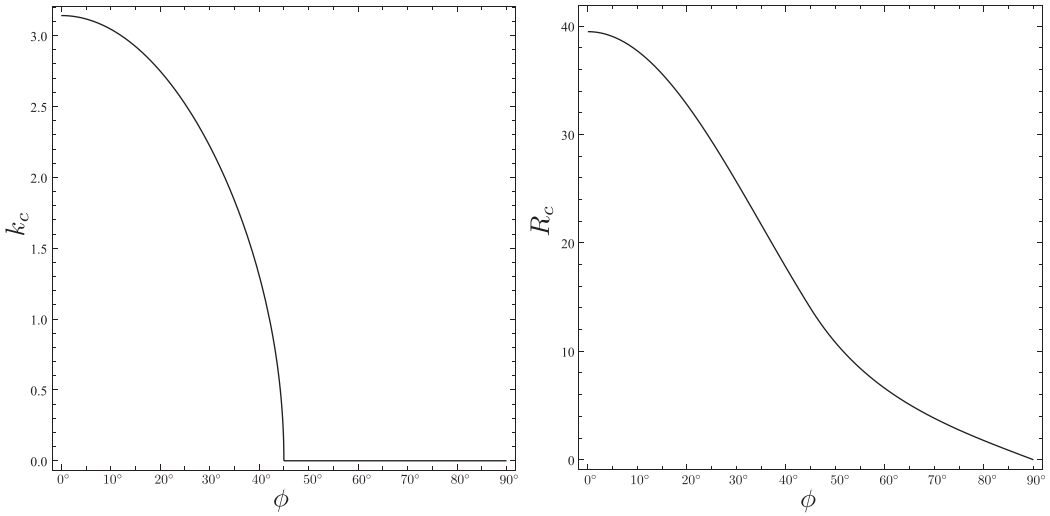

FIG. 9. Longitudinal rolls: Plots of k_c versus ϕ and R_c versus ϕ for the buoyancy–balanced rest state.

VI. OBLIQUE ROLLS

We now test the response of the basic solution Eqs. (5) to the normal modes with a wave vector arbitrarily oriented to the x–direction, namely the oblique rolls. In order to solve the linear disturbance equation for the oblique rolls, it is convenient to adopt a pressure representation of the velocity disturbance $\mathbf{U}$ instead of a streamfunction representation as for the longitudinal rolls. Thus, we express $\mathbf{U}$ as

$$\mathbf{U} = -\boldsymbol{\nabla} P + R\theta \left(\sin\phi \, \hat{\mathbf{e}}_x + \cos\phi \, \hat{\mathbf{e}}_y \right), \tag{34}$$

where P is the pressure disturbance. Eq. (34) implies that Eqs. (13) are reduced to the following pair of partial differential equations:

$$\nabla^2 P = R \left(\frac{\partial \theta}{\partial x} \sin\phi + \frac{\partial \theta}{\partial y} \cos\phi \right), \tag{35a}$$

$$\frac{\partial \theta}{\partial t} + u_b(y) \frac{\partial \theta}{\partial x} - \lambda \left(R\theta \sin\phi - \frac{\partial P}{\partial x} \right) - F(y) \left(R\theta \cos\phi - \frac{\partial P}{\partial y} \right) = \nabla^2 \theta. \tag{35b}$$

Eqs. (15) and (34) yield the boundary conditions

$$y = 0, 1 : \qquad \frac{\partial P}{\partial y} = 0, \quad \theta = 0. \tag{36}$$

In order to investigate the condition of neutral stability, we now consider the normal mode disturbances,

$$\begin{Bmatrix} P(x,y,z,t) \\ \theta(x,y,z,t) \end{Bmatrix} = \begin{Bmatrix} q(y) \\ h(y) \end{Bmatrix} \exp\left[i(kx\cos\gamma + kz\sin\gamma - \omega t)\right]. \tag{37}$$

Here, γ denotes the inclination angle of the disturbance wave vector to the x–direction. If $\gamma = 90^\circ$, we have the longitudinal rolls. If $\gamma = 0^\circ$, we have the transverse rolls. If $0^\circ < \gamma < 90^\circ$, we have the oblique rolls.

On substituting Eq. (37) into Eqs. (35) and (36), we obtain

$$q'' - k^2 q - Rh'\cos\phi - ikhR\cos\gamma\sin\phi = 0, \tag{38a}$$

$$h'' + \left[i\omega - k^2 + R_H\sin\phi + RF(y)\cos\phi - iku_b(y)\cos\gamma\right]h - F(y)q' - ik\frac{R_H}{R}q\cos\gamma = 0, \tag{38b}$$

$$y = 0, 1: \qquad q' = 0, \quad h = 0. \tag{38c}$$

Eqs. (38) can be solved as an eigenvalue problem. One must fix the values of (k, γ, ϕ, R_H) and determine the pair (ω, R) as the eigenvalue. The solution of the eigenvalue problem can be achieved numerically by employing the Runge–Kutta method and the shooting method (see, for instance, Barletta and Rees[23] for a detailed description).

The analysis of the oblique rolls is carried out starting from the longitudinal rolls ($\gamma = 90^\circ$) and seeking the solution of the eigenvalue problem by continuously decreasing the value of γ from 90° to 0°. At each step, viz. for each value of γ, we take as a first guess the solution obtained at the previous step, and the first guess for the case $\gamma = 90^\circ$ is the solution obtained with the collocation method of weighted residuals described in Sec. V A. In order to check if there exist more unstable branches of oblique rolls not continuously connected with the longitudinal rolls, we employ a search with randomly generated first guess data, with R smaller than the critical value for longitudinal rolls. No such branches were detected in all the cases examined.

We mention that one cannot in general reduce the analysis of the oblique rolls to that of the transverse rolls,[5] as it is indeed the case when $R_H = 0$. In other words, with $R_H \neq 0$, one cannot define a transformation that maps the three–dimensional linear stability analysis to an equivalent two–dimensional formulation.

For the buoyancy–balanced rest state, Eqs. (38) yield

$$q'' - k^2 q - Rh'\cos\phi - ikhR\cos\gamma\sin\phi = 0, \tag{39a}$$

$$h'' + \left(i\omega - k^2 + R\sec\phi\right)h - q' - ikq\cos\gamma\tan\phi = 0, \tag{39b}$$

$$y = 0, 1: \qquad q' = 0, \quad h = 0. \tag{39c}$$

A. Neutral stability and critical conditions

The main objective of the stability analysis relative to the oblique rolls is to ascertain if these disturbances are more or less dangerous than the longitudinal rolls hitherto considered. This study is carried out by comparing the critical values of R for general oblique rolls with those for the longitudinal rolls, for fixed values of R_H and ϕ. This study is carried out on the basis of Figs. 10–12 for upward–cooling basic flows ($R_H \geq 0$), of Fig. 13 for upward–heating basic flows ($R_H < 0$), and of Figs. 14 and 15 for the buoyancy–balanced rest state ($R_H = R\tan\phi$). In the latter case, only the inclination angle ϕ needs to be fixed. We mention that a general feature of the oblique rolls

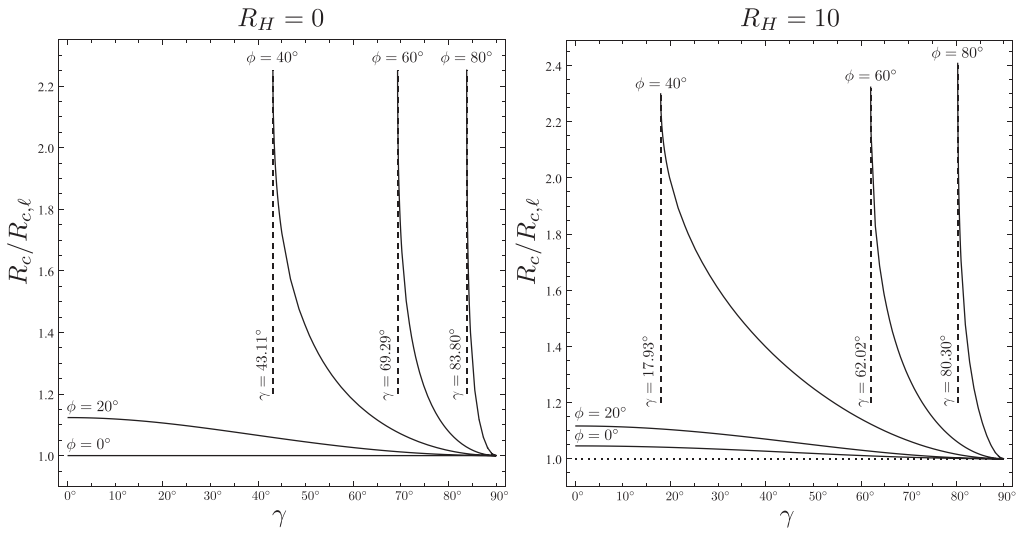

FIG. 10. Oblique rolls: Plots of $R_c/R_{c,\ell}$ versus γ with $R_H = 0$, 10, and different values of ϕ.

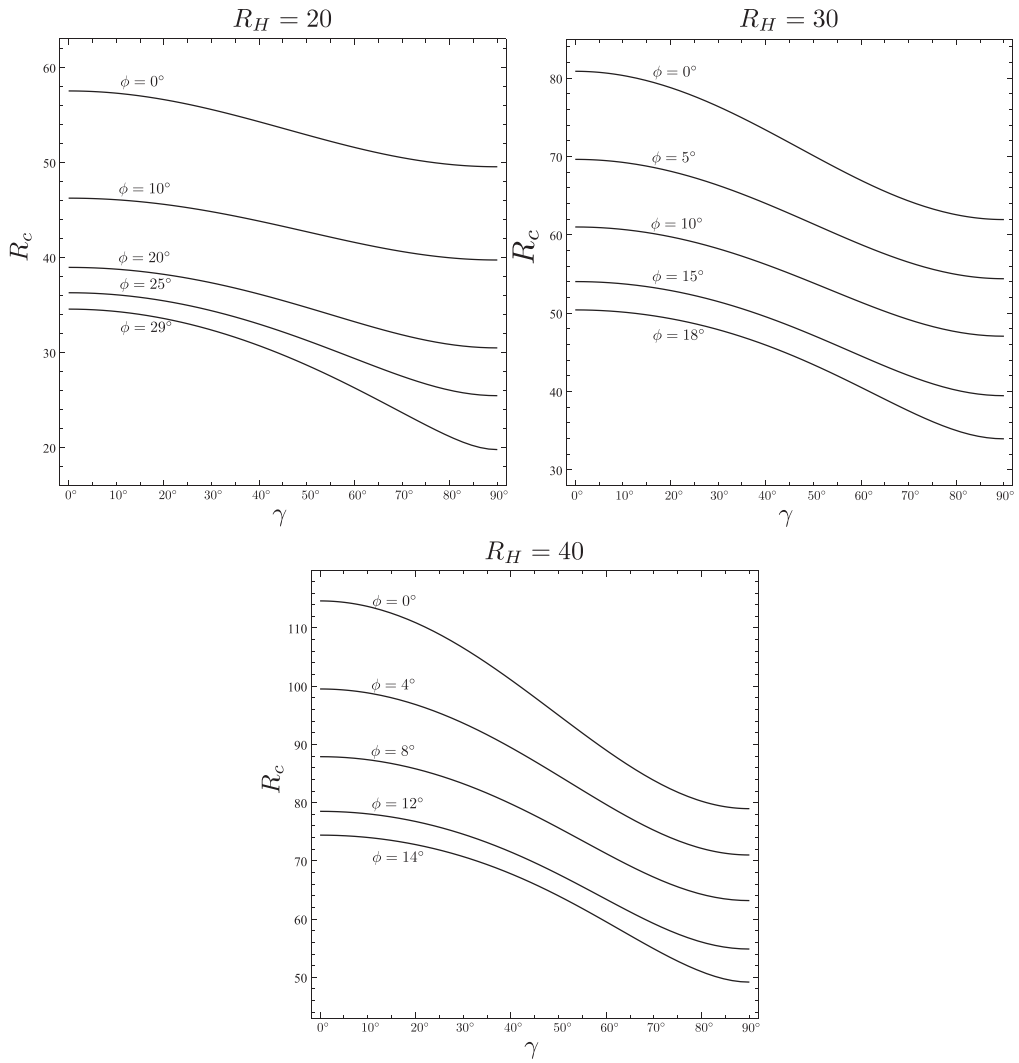

FIG. 11. Oblique rolls: Plots of R_c versus γ with $R_H = 20$, 30, 40, and different values of ϕ.

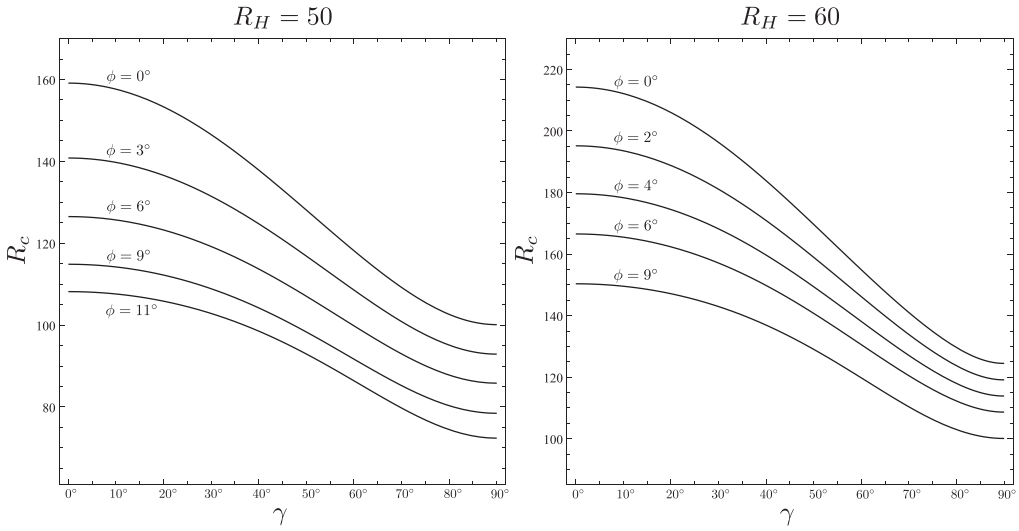

FIG. 12. Oblique rolls: Plots of R_c versus γ with $R_H = 50$, 60, and different values of ϕ.

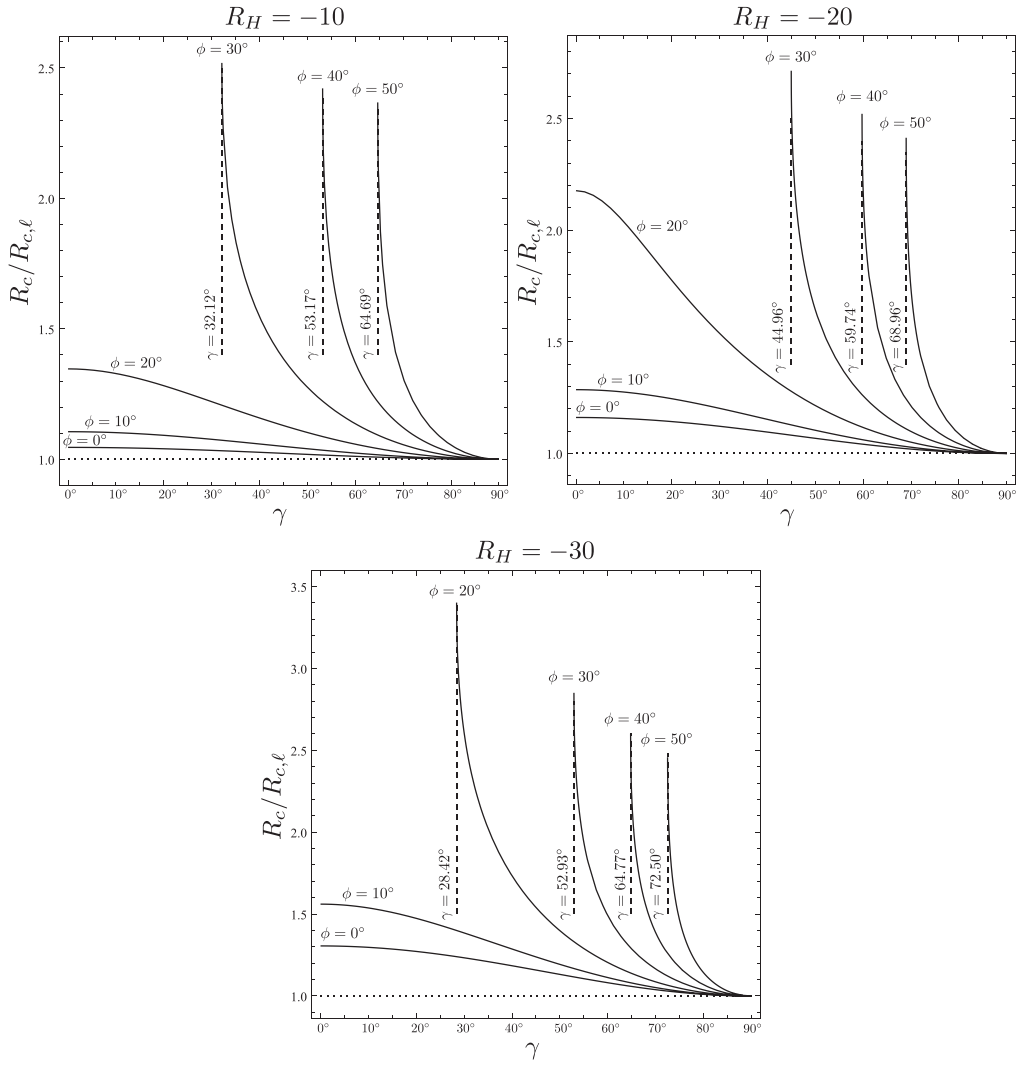

FIG. 13. Oblique rolls: Plots of $R_c/R_{c,\,\ell}$ versus γ with $R_H = -10$, -20, -30 and different values of ϕ.

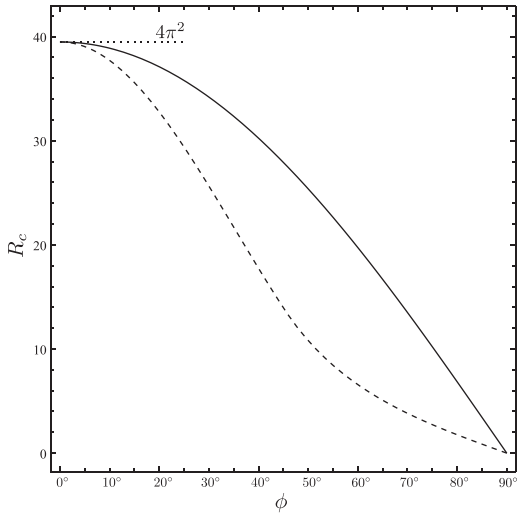

FIG. 14. Transverse rolls: Plot of R_c versus ϕ for the buoyancy–balanced rest state (solid line); the dashed line is the plot of R_c versus ϕ relative to the longitudinal rolls.

($\gamma < 90°$) and of the transverse rolls ($\gamma = 0°$) is being non–travelling modes ($\omega = 0$) in all the cases examined.

Figures 10–15 show that the longitudinal rolls are the most effective disturbances at the onset of the convective instability. This conclusion emerges clearly from the plots of R_c, or $R_c/R_{c,\ell}$, versus γ reported in Figs. 10–15. Here, the subscript ℓ stands for "longitudinal". The values of R_c at $\gamma = 90°$ are always smaller than those for $\gamma < 90°$. An exception is the case ($\phi = 0°$, $R_H = 0$) illustrated in Fig. 10 and in Figs. 14 and 15. In fact, this case is the classical Darcy–Bénard stability problem where $R_c = 4\pi^2$, and the angle γ does not influence the neutral stability condition due to the symmetry by rotations around the vertical y–axis.

Figure 10 is relative to $R_H = 0$, 10. The left and right frames of this figure reveal a qualitatively similar behaviour for $R_H = 0$ and $R_H = 10$. In particular both the left frame and the right frame show that, for $\phi = 40°$, $60°$, $80°$, the oblique rolls may exist only if γ is greater than a threshold value that depends on ϕ and R_H. In the case $R_H = 0$, Fig. 10 is perfectly consistent with the results of the

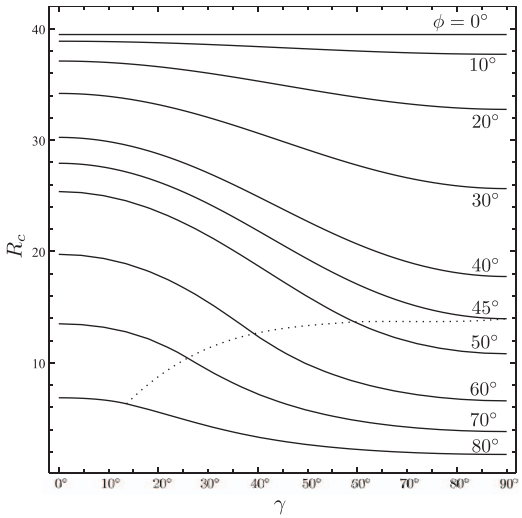

FIG. 15. Oblique rolls: Plots of R_c versus γ for the buoyancy–balanced rest state (solid lines) with different values of ϕ; the dotted line denotes the upper boundary of the region where the critical condition for the oblique rolls yields $k_c = 0$.

analysis carried out by Rees and Bassom.[5] These authors proved that the instability to oblique rolls is possible only if γ fulfils the inequality

$$\cos\gamma < \frac{0.612568}{\tan\phi}. \tag{40}$$

This means that, with $\phi = 40^\circ$, oblique rolls are allowed only for $\gamma > 43.11^\circ$. With $\phi = 60^\circ$ and $\phi = 80^\circ$, we have $\gamma > 69.29^\circ$ and $\gamma > 83.80^\circ$, respectively. No threshold angles γ exist with $\phi = 20^\circ$, because the inequality (40) is fulfilled for every value of γ in this case. A threshold angle γ exists only if the inclination of the layer above the horizontal is $\phi > 31.49^\circ$. These results are in perfect agreement with the data reported in the left frame of Fig. 10. The right frame of Fig. 10 shows that, with $R_H = 10$, the threshold values of γ are for smaller angles. Moreover, unlike the case $R_H = 0$, the ratio $R_c/R_{c,\ell}$ at the threshold values of γ changes with ϕ. In fact, the results reported by Rees and Bassom[5] for the case $R_H = 0$ imply that $R_c/R_{c,\ell} = 2.25278$, at the threshold values of γ corresponding to every inclination angle $\phi > 31.49^\circ$. The change in the shape of the neutral stability curves for the oblique rolls as γ decreases approaching its lowest value was described by Rees and Bassom,[5] for the case $R_H = 0$. Indeed, the neutral stability curves mutate from a concave upward shape to a closed loop eventually shrinking to a point and disappearing, when γ tends to its lowest value.

The features of the linear stability to oblique rolls discussed with reference to Fig. 10 are retrieved also in Fig. 13. This figure is relative to the upward–heating regime with $R_H = -10$, -20, -30. For the upward–heating regime, we infer that the minimum values of γ for the existence of oblique rolls increase with $|R_H|$. For example, by fixing $R_H = -30$, we observe a threshold value $\gamma = 28.42^\circ$ relative to $\phi = 20^\circ$ that was not present either for $R_H = -20$ or for $R_H = -10$. As $|R_H|$ increases, we report also an increasing variability of the ratio $R_c/R_{c,\ell}$ at the threshold values of γ.

Figures 14 and 15 are relative to the buoyancy–balanced rest state. Figure 14 shows that the transverse rolls are more stable than the longitudinal rolls for every inclination angle $0^\circ < \phi < 90^\circ$. Transverse and longitudinal rolls become equivalent in the limiting cases $\phi = 0^\circ$ and $\phi = 90^\circ$. Figure 15 illustrates how R_c changes with γ at different inclination angles ϕ. We start from the Darcy–Bénard limiting case $\phi = 0^\circ$, where all the oblique and transverse rolls yield critical conditions equivalent to the longitudinal rolls. When the layer is inclined to the horizontal, the longitudinal rolls result again to be the most unstable. In Sec. V C, with reference to the longitudinal rolls, we reported two different regimes as ϕ increases. A regime with $k_c > 0$ exists when $0^\circ \le \phi < 45^\circ$. A regime with $k_c = 0$, meaning a monotonic increasing neutral stability function $R(k)$, exists when $45^\circ \le \phi < 90^\circ$. Figure 15 shows that the condition $k_c = 0$ is extended also to some oblique rolls when $45^\circ \le \phi < 90^\circ$: those with a sufficiently large γ. Thus, the dotted curve in Fig. 15 interpolates the minimum values of γ, for different inclinations $\phi > 45^\circ$, such that the onset of convection takes place with $k_c = 0$.

VII. CONCLUSIONS

The stability of the Darcy–Hadley flow in an inclined porous layer has been analysed. The basic buoyant flow having a zero mass flow rate is induced both by the inclination above the horizontal and by the nonuniform boundary temperatures. Two possible regimes have been examined: the upward–heating condition where the boundary temperatures increase up the slope; the upward–cooling condition where the boundary temperatures decrease up the slope. A special case of upward–cooling condition arises when the basic temperature gradient becomes vertical. In this special case, denoted as buoyancy–balanced rest state, the basic solution is such that the temperature gradient is vertical and the velocity field is zero.

The linear stability of the basic solution has been analysed by solving the disturbance equations for the normal modes. The case of longitudinal rolls, that is the modes with a wave vector perpendicular to the basic velocity, has been first considered. The disturbance equations have been solved as an eigenvalue problem by a collocation method of weighted residuals, and by a Runge–Kutta solver for a validation in a few special cases. The numerical solution has lead to the neutral

stability condition, namely the function $R(k)$ defining the onset of the instability for a given wave number k of the normal mode. Here R is the Darcy–Rayleigh number associated with the transverse temperature difference between the boundaries. The neutral stability function $R(k)$ is both influenced by the Hadley–Rayleigh number, R_H, associated with the basic temperature gradient down the slope, and by the layer inclination angle above the horizontal, ϕ. The main results obtained are the following:

- In the upward–cooling case ($R_H > 0$), the increasing inclination above the horizontal tends to destabilise the flow. The basic solution may become unstable for every value of R, when the inclination angle ϕ becomes sufficiently large. When this happens, the neutral stability function $R(k)$ does not have a positive absolute minimum.
- In the upward–heating case ($R_H < 0$), the increasing inclination above the horizontal tends to stabilise the flow. The critical values (k_c, R_c), corresponding to the absolute minimum of the neutral stability function $R(k)$, are such that R_c increases both with ϕ and with $|R_H|$.
- The stability of the buoyancy–balanced rest state ($R_H = R\tan\phi$) could be studied analytically for the longitudinal rolls. The critical value R_c decreases with ϕ in this case, and the critical wave number k_c is zero for every $\phi \geq 45^\circ$.

The analysis of the stability to the longitudinal rolls has been extended by considering three-dimensional normal modes, such that the wave vector has an arbitrary inclination γ to the basic velocity. With the general normal modes, the pressure representation of the velocity disturbances has been adopted, and the eigenvalue problem for the neutral stability has been solved numerically by employing a Runge–Kutta solver. With $\gamma = 0^\circ$ we have the transverse rolls, and with $0^\circ < \gamma < 90^\circ$ we have the oblique rolls. In all the cases considered, the oblique and the transverse rolls have been found to be more stable than the longitudinal rolls ($\gamma = 90^\circ$). Thus, the selected patterns at the onset of the instability are the longitudinal rolls. An exception to this rule is the special case of the Darcy–Bénard problem, obtained by the limits $\phi \to 0^\circ$ and $R_H \to 0$. In the Darcy–Bénard problem, the symmetry by rotations around the vertical axis ensures that all the normal modes (transverse, oblique, longitudinal) are equivalent.

ACKNOWLEDGMENTS

This work was financially supported by Italian government, MIUR grant (Grant No. PRIN–2009KSSKL3).

APPENDIX: EXCHANGE OF STABILITIES

The proof of the exchange of stability is based on the technique developed by Pellew and Southwell[27] and recently employed by Nouri-Borujerdi, Noghrehabadi, and Rees.[28]

Since we are interested in the neutral stability condition, we set $\Im\mathrm{m}\{\omega\} = 0$ so that ω is to be considered as a real parameter. We note that Eqs. (19a) and (19c) imply

$$f''(0) = f''(1) = 0. \tag{A1}$$

Thus, on account of Eqs. (19c) and (A1), repeated integration by parts allows one to write the following:

$$\int_0^1 \bar{f} f'''' \, dy = \left[\bar{f} f'''\right]_0^1 - \int_0^1 \bar{f}' f''' \, dy = -\left[\bar{f}' f''\right]_0^1 + \int_0^1 |f''|^2 \, dy = \int_0^1 |f''|^2 \, dy, \tag{A2a}$$

$$\int_0^1 \bar{f} f'' \, dy = \left[\bar{f} f'\right]_0^1 - \int_0^1 |f'|^2 \, dy = -\int_0^1 |f'|^2 \, dy, \tag{A2b}$$

where the overline stands for complex conjugate.

Equations (19a) and (19b) can be collapsed into a single fourth–order differential equation,

$$f'''' - k^2 f'' + \left(i\omega - k^2 + R_H \sin\phi\right)\left(f'' - k^2 f\right) - Rk^2 F(y) f \cos\phi = 0. \tag{A3}$$

We multiply Eq. (A3) by $\bar{f}$ and then we integrate with respect to y in the interval [0, 1]. Hence, on account of Eqs. (A2), we obtain

$$\int_0^1 \left(|f''|^2 + k^2|f'|^2\right) dy + \left(k^2 - R_H \sin\phi\right) \int_0^1 \left(|f'|^2 + k^2|f|^2\right) dy$$
$$- Rk^2 \cos\phi \int_0^1 F(y)|f|^2\, dy - i\omega \int_0^1 \left(|f'|^2 + k^2|f|^2\right) dy = 0. \tag{A4}$$

Equation (A4) is a complex equation and it is satisfied if and only if both its real part and its imaginary part are zero. The imaginary part of Eq. (A4) is zero if

$$\omega \int_0^1 \left(|f'|^2 + k^2|f|^2\right) dy = 0. \tag{A5}$$

Equation (A5) implies that either f is identically vanishing or $\omega = 0$. The former possibility is not acceptable, and hence the exchange of stabilities is proved.

[1] S. A. Bories and M. A. Combarnous, "Natural convection in a sloping porous layer," J. Fluid Mech. **57**, 63–79 (1973).
[2] J. E. Weber, "Thermal convection in a tilted porous layer," Int. J. Heat Mass Transfer **18**, 474–475 (1975).
[3] J. P. Caltagirone and S. Bories, "Solutions and stability criteria of natural convective flow in an inclined porous layer," J. Fluid Mech. **155**, 267–287 (1985).
[4] D. Nield, "A note on convection patterns in an inclined porous layer," Transp. Porous Media **86**, 23–25 (2011).
[5] D. A. S. Rees and A. P. Bassom, "Onset of Darcy–Bénard convection in an inclined layer heated from below," Acta Mech. **144**, 103–118 (2000).
[6] D. A. Nield and A. Bejan, *Convection in Porous Media*, 3rd ed. (Springer-Verlag, New York, 2006).
[7] D. A. Nield, A. Barletta, and M. Celli, "The effect of viscous dissipation on the onset of convection in an inclined porous layer," J. Fluid Mech. **679**, 544–558 (2011).
[8] A. Barletta and L. Storesletten, "Thermoconvective instabilities in an inclined porous channel heated from below," Int. J. Heat Mass Transfer **54**, 2724–2733 (2011).
[9] D. A. S. Rees and A. Barletta, "Linear instability of the isoflux Darcy–Bénard problem in an inclined porous layer," Transp. Porous Media **87**, 665–678 (2011).
[10] C. T. Simmons, A. V. Kuznetsov, and D. A. Nield, "Effect of strong heterogeneity on the onset of convection in a porous medium: Importance of spatial dimensionality and geologic controls," Water Resour. Res. **46**, W09539, doi:10.1029/2009WR008606 (2010).
[11] J. E. Weber, "Convection in a porous medium with horizontal and vertical temperature gradients," Int. J. Heat Mass Transfer **17**, 241–248 (1974).
[12] D. A. Nield, "Convection in a porous medium with inclined temperature gradient," Int. J. Heat Mass Transfer **34**, 87–92 (1991).
[13] D. A. Nield, D. M. Manole, and J. L. Lage, "Convection induced by inclined thermal and solutal gradients in a shallow horizontal layer of a porous medium," J. Fluid Mech. **257**, 559–574 (1993).
[14] D. A. Nield, "Convection in a porous medium with inclined temperature gradient: additional results," Int. J. Heat Mass Transfer **37**, 3021–3025 (1994).
[15] P. N. Kaloni and Z. Qiao, "Non-linear stability of convection in a porous medium with inclined temperature gradient," Int. J. Heat Mass Transfer **40**, 1611–1615 (1997).
[16] D. A. Nield, "Convection in a porous medium with inclined temperature gradient and vertical throughflow," Int. J. Heat Mass Transfer **41**, 241–243 (1998).
[17] L. Brevdo and M. Ruderman, "On the convection in a porous medium with inclined temperature gradient and vertical throughflow. Part I. Normal modes," Transp. Porous Media **80**, 137–151 (2009).
[18] L. Brevdo and M. Ruderman, "On the convection in a porous medium with inclined temperature gradient and vertical throughflow. Part II. Absolute and convective instabilities, and spatially amplifying waves," Transp. Porous Media **80**, 153–172 (2009).
[19] A. Barletta and D. A. Nield, "Instability of Hadley–Prats flow with viscous heating in a horizontal porous layer," Transp. Porous Media **84**, 241–256 (2010).
[20] E. Diaz and L. Brevdo, "Absolute/convective instability dichotomy at the onset of convection in a porous layer with either horizontal or vertical solutal and inclined thermal gradients, and horizontal throughflow," J. Fluid Mech. **681**, 567–596 (2011).
[21] A. Barletta, M. Celli, and A. V. Kuznetsov, "Transverse heterogeneity effects in the dissipation-induced instability of a horizontal porous layer," ASME J. Heat Transfer **133**, 122601 (2011).
[22] A. Barletta, M. Celli, and A. V. Kuznetsov, "Heterogeneity and onset of instability in Darcy's flow with a prescribed horizontal temperature gradient," ASME J. Heat Transfer **134**, 042602 (2012).

[23] A. Barletta and D. A. S. Rees, "Local thermal non–equilibrium effects in the Darcy–Bénard instability with isoflux boundary conditions," Int. J. Heat Mass Transfer **55**, 384–394 (2012).
[24] D. A. S. Rees, "The stability of Darcy–Bénard convection," in *Handbook of Porous Media*, edited by K. Vafai, and H. A. Hadim (CRC, New York, 2000), Chap. 12, pp. 521–558.
[25] P. A. Tyvand, "Onset of Rayleigh–Bénard convection in porous bodies," in *Transport Phenomena in Porous Media II*, edited by D. B. Ingham and I. Pop (Pergamon, New York, 2002), Chap. 4, pp. 82–112.
[26] A. Barletta, "Thermal instabilities in a fluid saturated porous medium," in *Heat Transfer in Multi–Phase Materials*, edited by A. Öchsner and G. E. Murch (Springer, New York, 2011), pp. 381–414.
[27] A. Pellew and R. V. Southwell, "On maintained convective motion in a fluid heated from below," Proc. R. Soc. London A **176**, 312–343 (1940).
[28] A. Nouri-Borujerdi, A. R. Noghrehabadi, and D. A. S. Rees, "Influence of Darcy number on the onset of convection in a porous layer with a uniform heat source," Int J. Therm. Sci. **47**, 1020–1025 (2008).